

## ORGANIZATION OF ARM MOVEMENTS. MOTION IS SEGMENTED

J. F. SOECHTING\* and C. A. TERZUOLO†

Laboratory of Neurophysiology, Department of Physiology, 5-257 Millard Hall, University of Minnesota, Minneapolis, MN 55455, U.S.A.

**Abstract**—A kinematic analysis of human arm trajectories which underlie the production of learned, continuous movements (such as drawing of 'figure 8s' and stars) in free space is presented. The objective of this investigation was to see if a set of rules, which had been identified previously and which are appropriate for generating circular or elliptical motion of the wrist in an arbitrary plane, also hold true for arbitrary, learned trajectories provided one additional assumption is made: that apparently continuous complex movements are composed of unit segments.

The results presented in this paper are consistent with this hypothesis. Furthermore, as predicted by the hypothesis, the wrist trajectory deviates little from planar motion in each segment while the plane of motion can change abruptly from one segment to the next.

In a recent paper<sup>17</sup> we have considered a set of rules according to which simple trajectories (circles and ellipses) of the wrist can be generated in any arbitrary plane in free space. Also, a way was suggested for extending the use of this algorithm so as to encompass any arbitrary and complex trajectory that the human arm can execute in three-dimensional space.

In this paper and the one which follows<sup>18</sup> we address the latter point by considering first the case of highly learned trajectories (drawing of 'figure 8s' and stars) and, in the next paper, that of trajectories which either require careful planning or which are drawn extemporaneously.

To introduce this work it may be appropriate to recall briefly the main elements of the proposed algorithm as well as the assumptions which do allow one to generalize its use, i.e. to generate any arbitrary arm movement in space. We shall also restate the prediction which follows from these assumptions, the verification or falsification of this prediction being the major objective of these two papers.

To begin with, it was found experimentally that when subjects draw circles and ellipses in different planes of free space, the motion at the wrist as well as the motion for a chosen set of angles<sup>12,16</sup> describing the orientation of the upper arm and forearm are close to sinusoidal.<sup>15</sup> This set of angles is, in our hypothesis, the internal system of coordinates for movement co-ordination and perception (on the basis of kinesthetic information). The following relations between these angular motions (intrinsic parameters)

and the extrinsic parameters (the motion of the endpoint, i.e. the wrist) were identified:

(a) the azimuth of the plane of motion at the wrist is linearly related to the phase between the yaw angles of the upper arm and the forearm and

(b) the slant of the ellipse is linearly related to the phase between forearm yaw angle and the angular elevation of the arm.<sup>17</sup>

Also, and most importantly, the angular motions of the arm and forearm were found to be constrained in the following way: the phase difference between the modulation of the angular elevations of the arm and the forearm is close to 180°, independently of the plane in space in which the figures are drawn. As a result of this constraint the number of degrees of freedom of the arm is effectively reduced from four (three at the shoulder and one at the elbow, assuming that the center of rotation at the shoulder joint is fixed) to three. Thus, while in general there is no unique configuration of the arm which corresponds to a given wrist position, the constraint mentioned above introduces uniqueness in the relation between intrinsic and extrinsic parameters during a movement. Note also that simulation studies<sup>17</sup> have shown the following: when this constraint is satisfied, the other two rules are obeyed over a wide range of random combinations of angular motions. Thus, the rules are valid for generating circles and ellipses of different sizes, in different parts of space and in different planes.

Next, to make the algorithm applicable to arbitrary movements we suggested the following two assumptions, both of which are reasonable based on available experimental evidence:<sup>5,11,20–22</sup>

(1) apparently continuous, complex movements are composed of unit segments, and

\*To whom correspondence should be addressed.

†Dr Terzuolo is also affiliated with Istituto di Fisiologia dei Centri Nervosi, CNR, Milan, Italy.

(2) each of these segments is an arc of an ellipse generated according to the rules of the algorithm. We shall refer to the algorithm and these two assumptions as the 'hypothesis'.

The point to be stressed is the following: according to the hypothesis the motion of the wrist during each segment of a trajectory would, of necessity, lie in one plane only.<sup>17</sup> Indeed, the experimental verification or falsification of this prediction for different types of trajectories, both learned and novel, is obviously of crucial importance if the hypothesis is to be accepted as plausible and adequate.

In this paper we endeavor to show that learned trajectories as different as 'figure 8s' and stars can be accounted for by the hypothesis. In the subsequent paper<sup>18</sup> we will then present results obtained when subjects were asked to perform a novel task, namely to reproduce curved non-planar motion of the wrist.

### EXPERIMENTAL PROCEDURES

#### Motor tasks

Right-handed human subjects, who stood erect, were asked to draw simple figures such as an '8' or a star within a cube measuring 50 cm to a side. The approximate size of the figure and the plane in which it was drawn (for example, frontal or oblique) were also specified. They were asked to draw the figure repetitively at a comfortable tempo.

#### Recording system

The system used to record the motion of the arm in space and the analytical procedures used to calculate the angular motion at the shoulder and elbow have been described extensively in previous publications.<sup>14,15,17</sup> In brief, the locations of the elbow and of the wrist were determined ultrasonically and the flexion-extension at the elbow joint was measured goniometrically. From these measures the angular elevations ( $\theta$ ,  $\beta$ ) and yaw angles ( $\eta$ ,  $\alpha$ ) of the arm and forearm were calculated, the angular elevation of a limb segment being given by the angle between that segment and the vertical (measured in a vertical plane) while the yaw angle is defined in the horizontal plane relative to the anterior direction (Fig. 1). There is some uncertainty in the calculation of the yaw ( $\eta$ ) and angular elevation ( $\theta$ ) of the upper arm since the center of rotation at the shoulder does not remain stationary. One estimate of this error is given by the difference between the measured and calculated angle of elbow flexion; the root mean square difference between these values ranged from 2° to 4°.

Wrist and hand motion were not measured. Given the amplitude of the movements investigated, the contribution to the motion by these distal joints is negligible. For example, during handwriting on a horizontal surface<sup>7</sup> the amplitude of wrist rotation is generally limited to a few degrees and the velocity of the motion at the finger tip is highly correlated with that at the wrist. Furthermore, in the experiments to be reported here subjects were asked to perform the task while keeping their wrist rigid.

Electromyographic activity of shoulder and elbow muscles was recorded conventionally using surface electrodes.

#### Data analysis

For purposes of analysis we assumed that arm motion consisted of distinct segments and that each segment began and ended at an extremum (maximum or minimum) of the tangential velocity of the wrist. The reasons for defining segments in this arbitrary manner are as follows. First, the tangential velocity ( $V_T$ ) at the wrist was not constant during

a movement; rather it exhibited a considerable amount of modulation (cf. Fig. 2). In the absence of any compelling reasons to the contrary, one might thus choose the extrema of  $V_T$  to define a segment. Second, in agreement with previous observations<sup>1,2,8,22</sup> as well as one assumption of the hypothesis being tested, the tangential velocity was found to be inversely related to the curvature  $\kappa$  of the motion at the wrist (cf. Fig. 2). For a 'figure 8' the curvature is at a minimum at the point of inflection of the curve, that is, where the motion changes from clockwise to counter-clockwise, or vice versa. Since a 'figure 8' can be approximated by two ellipses, one above the other, the point of inflection constitutes an obvious choice of a segment boundary. Similarly, for a 'star', the curvature is maximal at each corner and one might expect each stroke to constitute a segment. Finally, a detailed investigation has shown that the curvature is proportional to the inverse of the cube of the velocity<sup>8,21</sup> (or equivalently, that the angular velocity is proportional to the curvature to the 2/3 power). In this work, it was found that the slope of this relationship can change abruptly, the change occurring always at points of inflection and usually at a minimum of the curvature. One way of interpreting this observation is that such a change in the constant of proportionality defines the beginning of a new segment.

Curvature was calculated numerically.<sup>19</sup> The velocity of the wrist is given by

$$\mathbf{V} = V_T \mathbf{t} \quad (1)$$

where  $\mathbf{t}$  is the tangent vector of unit length. The curvature  $\kappa$  can then be calculated from

$$\kappa = \left| \frac{d\mathbf{t}}{dt} \right| / V_T \quad (2)$$

that is, the time rate of change of the tangent vector divided by the tangential velocity. Velocity was obtained by numerical differentiation of the wrist position data following double-sided exponential smoothing.

Sinusoids were fitted to the X, Y and Z components of wrist velocity as well as to the velocities of the orientation angles (yaw and angular elevation) of the arm and forearm. The period of the sinusoidal oscillations in a given segment could differ from its duration and could vary from segment

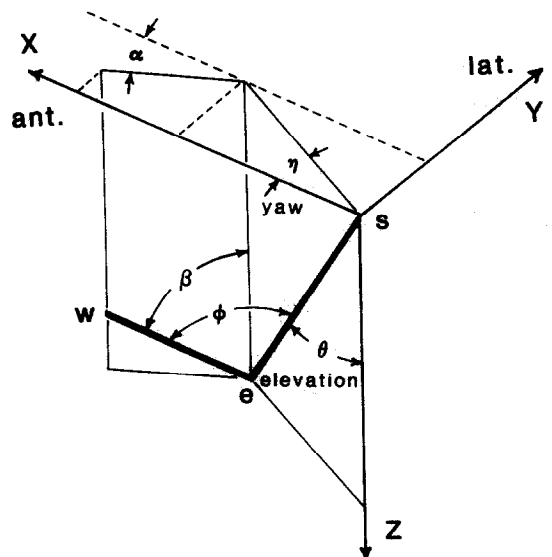


Fig. 1. Parameters used to define the angular orientation of the arm. The angles  $\theta$  and  $\beta$  represent the angular elevation of the arm and forearm, while the yaw angles are given by  $\eta$  and  $\alpha$ .

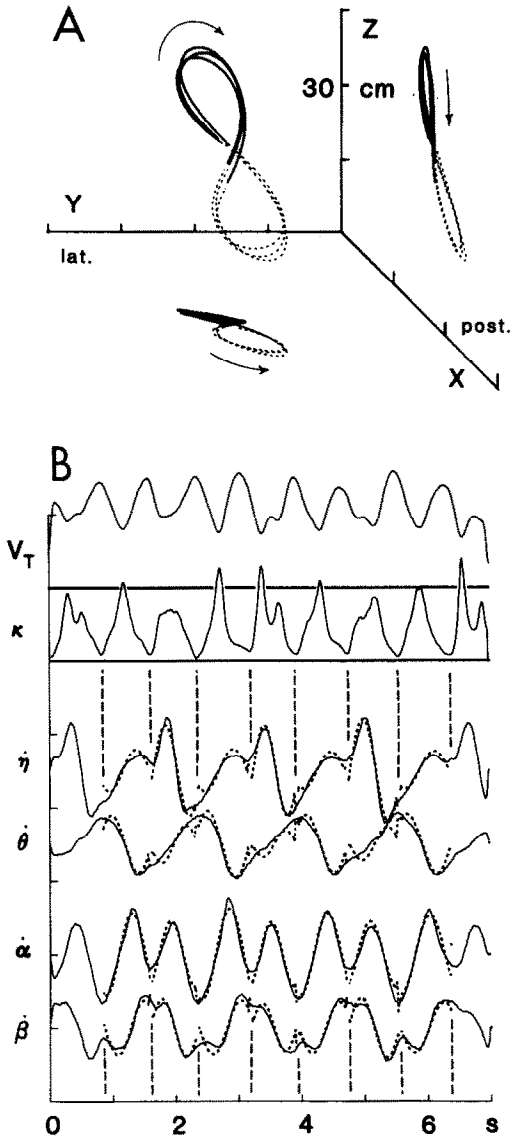


Fig. 2. (A) Plot (as viewed from the perspective of subject) of the trajectory of the wrist in three-dimensional space and its projection on the horizontal and sagittal planes. This movement was assumed to consist of two segments; one is denoted by the solid traces, the other by the dashed lines. The arrows indicate the direction of motion. (B) Tangential velocity  $V_T$  and the curvature  $\kappa$  of the wrist motion as well as the angular velocities of the upper arm ( $\eta$ , yaw;  $\theta$ , angular elevation) and of the forearm ( $\alpha$ , yaw; and  $\beta$ , elevation). The vertical dashed lines coincide with the minima of the curvature and denote the beginning and end of a segment. Sinusoids were fitted to the angular velocities over each segment; they are indicated by dashed lines. The scale in (B) is per division:  $V_T$ , 50 cm/s;  $\kappa$ , 0.25/cm; angular velocities, 250°/s.

to segment. The period was therefore chosen to minimize the sum of the distortions from sinusoidal motion of the velocities of the orientation angles. Distortion was defined conventionally as the root mean square difference between the fundamental component and the experimental value, normalized by the latter's variance. It can thus range from 0 to 1.

#### Determination of the plane of motion

The instantaneous plane of motion of the trajectory of the wrist can be computed from its velocity and acceleration. The velocity is tangential to the trajectory (1), while the acceleration has tangential and perpendicular components. The velocity and acceleration vectors together define the instantaneous plane of motion, that is, the perpendicular to the velocity and acceleration vectors (the binormal) is perpendicular to the plane of motion. Thus

$$\mathbf{n} = \mathbf{V} \times \mathbf{A} \quad (3)$$

where  $\mathbf{n}$  is the binormal and the right side is the vector cross-product of velocity and acceleration. The components of  $\mathbf{n}$  are given by

$$\begin{aligned} n_x &\simeq v_y a_z - v_z a_y \\ n_y &\simeq v_z a_x - v_x a_z \\ n_z &\simeq v_x a_y - v_y a_x \end{aligned} \quad (4)$$

where  $X$ ,  $Y$  and  $Z$  are the axes of a Cartesian coordinate system defined by the right-hand rule. We also calculated the planar elevation  $\psi$  and azimuth  $\chi$  of the plane of motion according to

$$\begin{aligned} \tan \chi &= n_y/n_x \\ \tan \psi &= -n_z/\sqrt{(n_x^2 + n_y^2)} \end{aligned} \quad (5)$$

where  $x$  is in the anterior direction,  $y$  in the lateral direction and  $z$  is downward.

For each segment we computed the plane of motion in two ways:

- (1) by calculating the average value for  $\mathbf{n}$  (4) over that segment and
- (2) by linear regression. Since the equation of the plane in a given segment is

$$n_x x + n_y y + n_z z = a \quad (6)$$

we calculated  $\mathbf{n}$  and  $a$  to give the best fit of the wrist trajectory to (6) in a least-square sense.

Finally, as a help in presenting the data we found it convenient to define another coordinate system in which the motion of a chosen segment of trajectory lies in the plane  $x' = \text{constant}$ . This coordinate system results from two successive rotations:

- (1) by an angle  $\chi$  about the vertical axis and
- (2) by an angle  $\psi$  about the  $Y$ -axis defined after the first rotation. The two coordinate systems are related by

$$\begin{Bmatrix} x' \\ y' \\ z' \end{Bmatrix} = \begin{bmatrix} \cos \psi \cos \chi & \cos \psi \sin \chi & -\sin \psi \\ -\sin \chi & \cos \chi & 0 \\ \sin \psi \cos \chi & \sin \psi \sin \chi & \cos \psi \end{bmatrix} \begin{Bmatrix} x \\ y \\ z \end{Bmatrix} \quad (7)$$

The wrist trajectory was rotated into this coordinate system using (7) and the deviation from planar motion ( $\epsilon$ ) was quantified by

$$\epsilon = \left\{ \sum v_x^2 / (v_y^2 + v_z^2) \right\}^{1/2} \quad (8)$$

where  $v_x$  is the out-of-plane component of the velocity and  $v_y$  and  $v_z$  are the in-plane components.

## RESULTS

Figure 2 shows typical results obtained when subjects were asked to draw a 'figure 8' with their right arm. The upper panel (Fig. 2A) shows a perspective view of the path taken by the wrist in the performance of this task in three successive cycles, while Fig. 2B illustrates the changes in tangential velocity

( $V_T$ ) and curvature ( $\kappa$ ) of the wrist trajectory, as well as the modulation in velocity of the orientation angles of the upper arm (yaw,  $\eta$ ; angular elevation,  $\theta$ ) and of the forearm (yaw,  $\alpha$ , angular elevation,  $\beta$ ).

In Fig. 2, the subject was asked to draw the figure in the frontal ( $Y-Z$ ) plane (the height of the figure drawn being about 35 cm). The velocity of the wrist was not constant during the execution of the movement, ranging from 37 to 80 cm/s and was negatively correlated with the curvature  $\kappa$  which ranged from 0.03 to 0.32/cm. For the reasons detailed in Experimental Procedures, we assumed that the movement consisted of distinct segments and that a new segment began when velocity was at a maximum and curvature was at a minimum. Thus, one segment of the trajectory corresponds to the upper loop of the 'figure 8' while the other corresponds to the lower loop. This may be appreciated in the perspective view of the wrist trajectory (as well as its projection on the sagittal and horizontal planes) in Fig. 2A, where the two segments are represented by solid and dashed lines, respectively.

Segment boundaries are also indicated in Fig. 2B by the vertical dashed lines. A sinusoid was fitted in each segment to each of the angular velocities, that is upper arm yaw ( $\eta$ ) and elevation ( $\theta$ ) and forearm yaw ( $\alpha$ ) and elevation ( $\beta$ ). The dashed traces show this fundamental component while the solid traces represent the experimental data. The sinusoids gave a good fit to the data except in the vicinity of the segment boundaries. At these boundaries the sinusoidal velocity was not infrequently discontinuous, while the experimentally obtained velocities

showed no such discontinuities. (Note that a discontinuity in velocity cannot be realized physically since it implies that acceleration and torque are infinite at that point.) The average distortion of the angular velocities from sinusoidal modulation over each segment ranged from 22% for forearm yaw ( $\alpha$ ) to 41% for upper arm elevation ( $\theta$ ). The standard deviation of the difference between the simulated and experimental angular displacements ranged from 1.4 to 2.9° in this trial.

The ability of such a piecewise sinusoidal approximation to capture the main features of the movement can be appreciated in Fig. 3. The upper row of this figure shows experimental data for the same trial as depicted in Fig. 2, while the lower row shows the results obtained when the motion of the wrist was computed assuming the angular motion of the upper arm and forearm to be sinusoidal in each segment. The panels show the projection of wrist motion on the frontal plane and the covariations between orientation angles.

When subjects are asked to draw circles and ellipses in different planes, we had found previously<sup>15,17</sup> that the modulation of angular elevation of the forearm ( $\beta$ ) was about 180° out of phase with that of the upper arm ( $\theta$ ), with a standard deviation of about 25°. Moreover, when the motion was close to the frontal plane (azimuth  $\chi \approx 0^\circ$ ), the two yaw angles ( $\eta$  and  $\alpha$ ) were modulated approximately in phase with each other (with a range of  $\pm 30^\circ$ ). Finally, the slant of the ellipse ( $\sigma$ ) was found to be highly correlated with the phase difference between forearm yaw and elevation.

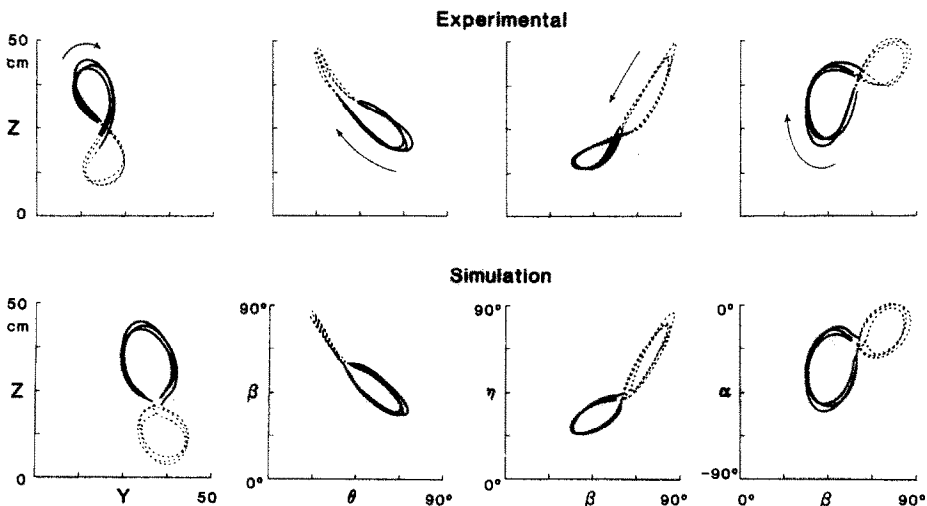


Fig. 3. The top row shows experimental data for the same trial as shown in Fig. 2. The panels depict the projection of the wrist trajectory on the frontal plane and angle-angle plots of the orientation angles; the two angular elevations ( $\theta$ ,  $\beta$ ) and upper arm yaw ( $\eta$ ) and forearm yaw ( $\alpha$ ) as a function of forearm angular elevation ( $\beta$ ). The lower row shows only the fundamental component (sinusoid) of the modulation of the orientation angles and the motion of the wrist which would result from such a sinusoidal modulation, assuming the length of the arm and forearm to be 30 cm. The solid traces and dashed lines denote the two segments constituting this motion, as defined in Fig. 2. The data points corresponding to the boundary between adjacent segments have been omitted in the simulations.

The phase relations among the orientation angles which hold for the segments of the 'figure 8' are not too different from those reported above. They are not always identical for the two segments, however. For example, for the trial illustrated in Figs 2 and 3, in the lower loop  $\beta$  led  $\theta$  by  $185 \pm 5^\circ$ . However, the phase lead in the upper loop, while still within the range of values found for circles and ellipses, was significantly less ( $144 \pm 3^\circ$ ). This can be appreciated in Fig. 3. During the dashed portion of the plot of  $\beta$  vs  $\theta$ , the relationship between these two variables is close to rectilinear, as would be expected if they were  $180^\circ$  out of phase, while the solid portion describes an ellipse. Also, in the upper loop  $\eta$  lagged  $\alpha$  by  $29 \pm 2^\circ$  while it led by  $44 \pm 5^\circ$  in the lower loop. In this trial, the coefficient of correlation between slant ( $\sigma$ ) and the phase difference between forearm yaw ( $\alpha$ ) and angular elevation ( $\beta$ ) was 0.998.

For the most part the data illustrated in Figs 2 and 3 are representative of the results obtained from three subjects when they were asked to draw 'figure 8s' in the frontal plane or in oblique planes. In most cases, wrist velocity was maximal (and the curvature  $\kappa$  at a minimum) when the two loops of the 'figure 8' crossed. In some instances, however, there was another maximum of the velocity in the middle of one or both of the loops and a corresponding minimum of the curvature. That is, one or both of the loops were flattened at the top or the bottom. In those cases we also assumed that each segment was demarcated by a maximum of the velocity, one complete cycle of the motion now requiring three or four segments (see Fig. 7).

In two of the three subjects the phase relations among the orientation angles were as shown in Fig. 3. The changes in angular elevations of the arm and forearm were close to  $180^\circ$  out of phase ( $\beta$  led  $\theta$  by  $174 \pm 31^\circ$ ,  $N = 104$  segments, in one subject, and by  $181 \pm 34^\circ$ ,  $N = 42$ , in the other subject). For the third subject, this phase difference was substantially different from  $180^\circ$  ( $139 \pm 45^\circ$ ,  $N = 34$ ) and also substantially different from the results obtained when he was asked to draw circles and ellipses ( $196 \pm 23^\circ$ ,  $N = 15$ ). In all three subjects, the slant ( $\sigma$ ) of each segment was highly correlated with the phase difference between  $\beta$  and  $\alpha$  (correlation coefficient  $r$  ranging from 0.975 to 0.989).

The analysis of the kinematic aspects of the data so far considered brought to light the presence of one characteristic common to all trials. While each segment defined a close-to-planar trajectory, the plane of motion of adjacent segments could differ appreciably. This can be ascertained by inspection of Fig. 2A. The upper loop (solid traces) lies in a plane which is close to the vertical since its projection on the horizontal plane describes a straight line. On the contrary, the lower loop is inclined with respect to the vertical, its projection on the horizontal plane describing an ellipse. (Note that this finding was not conditioned explicitly in the way the task was defined. On the

contrary, in the request to 'draw a figure 8' it is implicit that it be drawn in one plane.)

To characterize this observation more precisely we computed the instantaneous normal to the plane of motion in the manner described in Experimental Procedures. The components ( $n_x$ ,  $n_y$ ,  $n_z$ ) of this vector of unit length are shown in Fig. 4A for the same trial illustrated in Figs 2 and 3. From the normal vector we also calculated the planar elevation ( $\psi$ ), that is the inclination of the plane of motion with the vertical, and the azimuth ( $\chi$ ), that is the angle of the plane of motion relative to the sagittal plane. A negative value of  $\psi$  indicates that the upper portion of the plane is anterior to the lower portion. A positive value of  $\chi$  indicates the anterior portion of the plane is to the left of its posterior portion.

The results presented in Fig. 4A reinforce the conclusion drawn by visual inspection from the plot of Fig. 2A. For the upper loop the plane of motion lies close to the vertical, since  $\psi$  is close to zero (for example between 0.85 and 1.6 s), and it changes abruptly in the lower loop where  $\psi$  becomes negative (for example between 1.6 and 2.35 s). This can also be appreciated by inspection of the vertical component ( $n_z$ ) of the normal to the plane of motion, which is by definition zero when the plane of motion is vertical. The component of the normal in the anterior-posterior direction ( $n_x$ ) reverses sign as the movement changes from a clockwise direction to counter-clockwise. (For clockwise rotation in the frontal plane the normal points in the anterior direction and  $n_x$  is negative.) The direction of the movement changes when the curvature  $\kappa$  is at a minimum, that is at the point of junction of two segments as we have defined them.

For each segment we calculated the average plane of motion, as indicated by the dashed lines in Fig. 4A. We then rotated the wrist trajectory, using the coordinate transformation given in Experimental Procedures by (7), so that a given segment would lie in the plane  $x' = \text{constant}$ . The results of this operation are shown in Fig. 4B. The plot on the left in each row shows the projection of the wrist motion on the  $x'-z'$  plane (i.e. an edgewise view). The heavy, solid lines denote the segment which on average lies in the  $x' = \text{constant}$  plane, the dashed lines the preceding and succeeding segments. The extent to which the curve describing a given segment deviated from planar motion, that is  $\epsilon$ , was calculated as described in Experimental Procedures. For the two segments illustrated in Fig. 4B,  $\epsilon$  was 0.082 (top row) and 0.067 (bottom). For the seven segments which were analyzed for this trial,  $\epsilon$  averaged 0.086. In each case, the greatest deviation from planar motion occurred close to the boundary between adjacent segments.

In this trial the change in the orientation of the plane of motion from one segment to the next was substantial: in the upper loop of the 'figure 8', the planar elevation  $\psi$  was  $-4 \pm 2^\circ$  (average of four segments), while it was  $-25 \pm 2^\circ$  for the lower loop

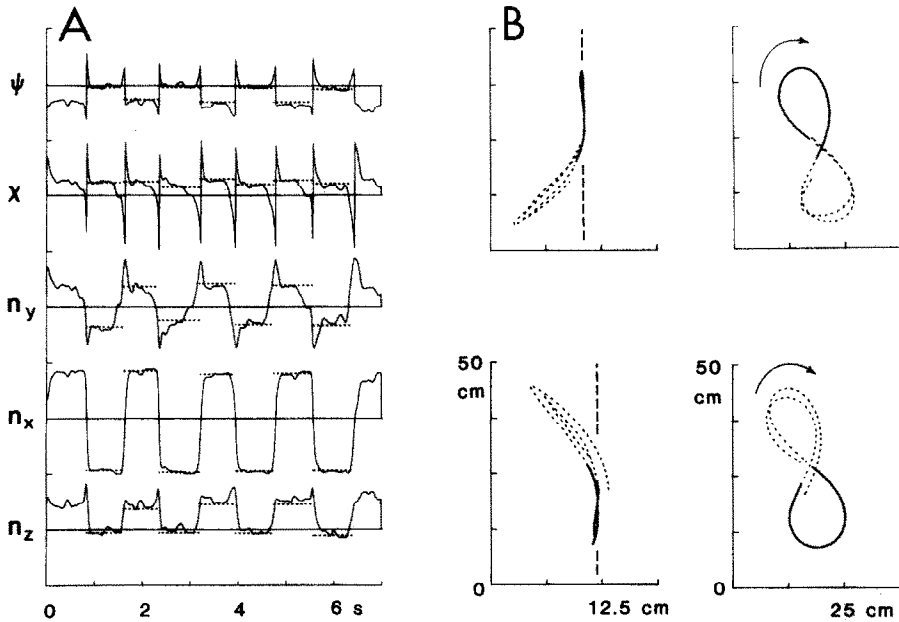


Fig. 4. (A) Variation in the instantaneous normal to the plane of motion and the two angles which can be used to define it ( $\psi$ —planar elevation and  $\chi$ —azimuth) for the same trial as shown in Figs 2 and 3. The  $x$ -component of the normal points in the posterior direction,  $n_y$  to the left and  $n_z$  upwards.  $n_x$  reverses sign when wrist motion changes from clockwise to counter-clockwise, i.e. at the beginning of a new segment. The dashed lines indicate the best fit to planar motion for each segment. Scale per division: direction normals ( $n_x, n_y, n_z$ )—1,  $\psi$  and  $\chi$ — $90^\circ$ . (B) Extent to which each segment deviates from planar motion. Wrist trajectory was rotated into the plane  $x' = \text{constant}$  and the leftmost plot in each row shows the projection of the trajectory onto the  $x'-z'$  plane (edgewise view) while the rightmost plot shows a head-on view ( $y'-z'$  plane). The vertical dashed lines are provided for reference and denote the plane of motion of the segment indicated by solid traces. The dashed portions of the curve depict the trajectories of the preceding and succeeding segments. Note that the  $x'$  scale has been expanded.

(three segments). The change in the azimuth  $\chi$  of the plane of wrist motion was much less in this trial ( $\chi = 19 \pm 3^\circ$  in the upper loop,  $25 \pm 2^\circ$  in the lower loop). This trial was not atypical of the results obtained from three subjects when we asked them to draw 'figure 8s' in the frontal plane or in oblique planes. For these subjects, in 23–37% of the cases, planar elevation  $\psi$  changed by more than  $20^\circ$  from one segment to the next, the average change ranging

from  $14$  to  $18^\circ$ . As for the azimuth  $\chi$ , it changed by more than  $20^\circ$  in 9–31% of the instances, with an average ranging from  $10^\circ$  to  $17^\circ$ . The deviation from planar motion for each segment ( $\epsilon$ ) averaged from  $0.071 \pm 0.025$  to  $0.098 \pm 0.051$  for the three subjects.

The results presented in Figs 2–4 concerning 'figure 8s' can be summarized as follows: If it is assumed that the wrist trajectory consists of discrete segments, each beginning and ending when the curvature of the

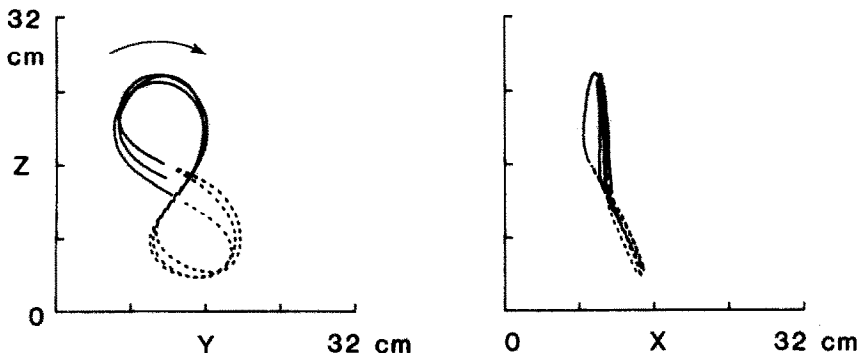


Fig. 5. The projection of wrist trajectory onto the frontal plane (left) and sagittal plane (right). Note the abrupt change in the plane of motion between the upper and lower segments of the 'figure 8'.

trajectory is at a minimum, then the modulation in the orientation angles of the arm and forearm can be adequately approximated as sinusoidal. The phase relations among the orientation angles and their correlation with parameters characterizing the wrist trajectory (plane of motion, slant) were for the most part close to those found previously when subjects were asked to draw circles and ellipses. Finally, the plane of motion of the wrist can change rather abruptly at the boundary between segments but remains fairly constant within each segment.

Figures 5 and 6 provide two more illustrations of these findings. Figure 5 illustrates another 'figure 8', which the subject was asked to draw in smaller size (22 cm in height, 1/3 smaller than the trial in Fig. 2). The projection of the wrist motion on the sagittal plane in the right panel shows clearly the abrupt change in the plane of wrist motion at the boundary between the two segments, making this feature independent from size.

Figure 6 illustrates a trial in which the subject was asked to draw a 'figure 8' in an oblique plane. As can be seen from the projection of wrist motion on the horizontal plane in the perspective plot (Fig. 6A) and from the plot of planar elevation ( $\psi$ ) in Fig. 6B, the upper loop of the figure was in a vertical plane,  $\psi$  being close to zero, while the lower loop has a

substantial inclination ( $\psi$  ranging from  $-25^\circ$  to  $-30^\circ$  for different segments). In this trial, the azimuth of the plane of wrist motion was also found to change by as much as  $25^\circ$  from one segment to the next.

We also asked subjects to draw a 'figure 8' lying on its side, that is ' $\infty$ '. The results for this task are shown in Figs 7-9. The curvature of the wrist trajectory reached a minimum and the velocity a maximum in the middle of each loop as well as at the point of inflection, where the motion changes from clockwise to counter-clockwise (Fig. 7). Therefore, according to the criteria for segment identification one cycle of the motion consists of four segments; they are denoted by the different line symbols in Fig. 7A and their boundaries are indicated by the dashed lines in Fig. 7B. Sinusoids gave a good fit to the modulation in the angular velocities in each segment and were able to reproduce quite well the figural aspects of the motion (compare the upper and lower rows of Fig. 8A). Also, the angular elevations of the arm ( $\theta$ ) and forearm ( $\beta$ ) were close to  $180^\circ$  out of phase. For the two subjects who performed this task this phase difference averaged  $168 \pm 31^\circ$  ( $N = 67$  segments) for one subject and  $188 \pm 19^\circ$  ( $N = 51$ ) for the other. In both cases the slant  $\sigma$  of each segment was highly correlated with the phase difference between forearm yaw ( $\alpha$ ) and angu-

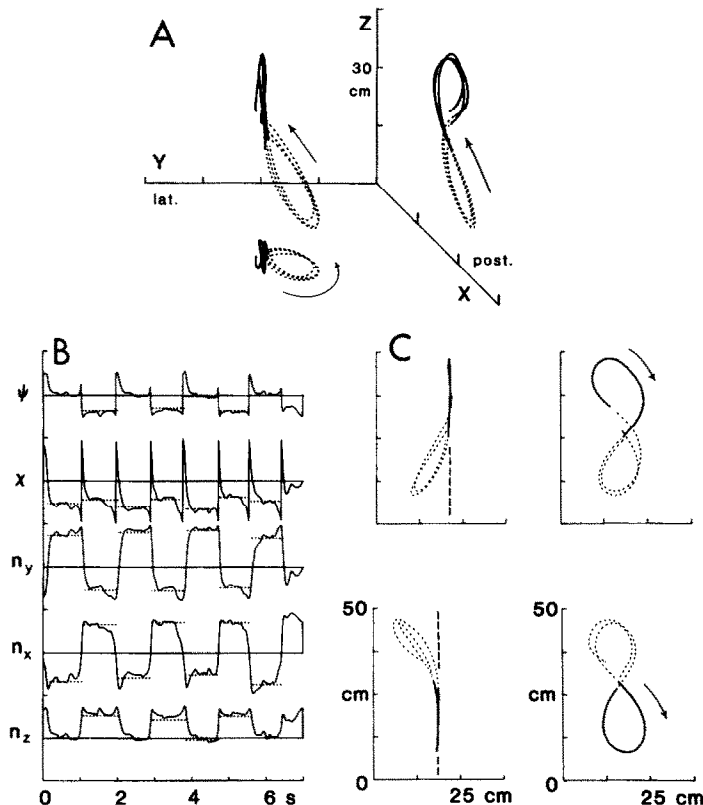


Fig. 6. A 'figure 8' drawn in an oblique plane. The format and scales of (A) to (C) are the same as in Figs 2 and 4.

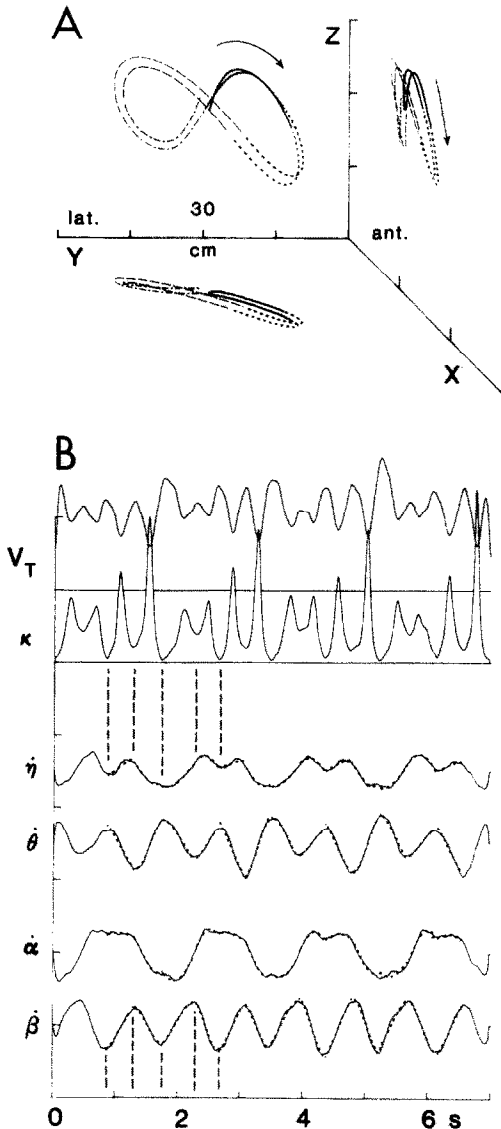


Fig. 7. (A) Trajectory of the wrist for a trial in which the subject was asked to draw  $\infty$ . Based on the modulation in the tangential velocity of the wrist, four segments were assumed for this trial. They are denoted by the different line symbols. (B) Variation in tangential velocity  $V_T$  and curvature  $\kappa$  and the angular velocities of the arm and forearm for the same trial. The vertical dashed lines indicate the four segments for the first cycle of the movement, beginning with the solid portion (first clockwise segment) in (A). Scales per division are:  $V_T$ , 50 cm/s;  $\kappa$ , 0.25/cm; angular velocities,  $200^\circ/\text{s}$ .

lar elevation  $\beta$  ( $r = 0.989$  and  $0.969$ ). Finally, as may be seen in Fig. 9, the plane of wrist motion can change abruptly even in the middle of one loop, that is at minima in the curvature which do not correspond to a point of inflection. For example, in the segment extending from 3.5 to 3.95 s,  $n_x = 0.91$ ,  $n_y = 0.37$  and  $\chi = 22^\circ$  while in the subsequent segment (from 3.95 to 4.35 s)  $n_x = 0.99$ ,  $n_y = 0.09$  and  $\chi = 5^\circ$ .

The assumption that the trajectory of apparently

continuous wrist motion consists of distinct segments and that the modulation of the orientation angles of the arm is sinusoidal within each segment should also account for rectilinear wrist motions, according to the hypothesis. To ascertain this point we asked subjects to draw simple figures consisting of straight line segments, such as a five-pointed star. In this case it seems reasonable to assume that each segment is terminated when the curvature reaches a maximum, that is at the corners of the star.

The results for one trial are illustrated in Figs 10 and 11. Figure 10 presents a comparison of the experimental data with the results of the simulation in which the angular motion was sinusoidal in each segment. The projection of wrist motion on the frontal plane and the co-variations of the orientation angles are shown. The simulation captures the form of the experimental data, including the curvature of some of the strokes which make up the star. As was the case for the other figures, the angular elevations of the arm and forearm were close to  $180^\circ$  out of phase on average ( $176 \pm 22^\circ$  and  $-173 \pm 48^\circ$  for the two subjects) and the slant of each segment was highly correlated with the phase difference between forearm yaw and angular elevation ( $r = 0.885$  and  $0.817$ ). The plane of motion in each segment cannot be estimated reliably for this task since each of the segments was close to rectilinear.

As a last point we wish to consider briefly movement dynamics. So far we have shown that a segmentation of apparently continuous movements is apparent in the kinematic characteristics of the distal motion and in the angular motions at the shoulder and elbow joints. One could thus expect to find evidence for such a segmentation also in the dynamic characteristics of the movement, namely the torques acting at the shoulder and elbow joints which are responsible for generating the movement as well as in the pattern of activation of muscles which contribute to produce those torques. Therefore, in one subject we recorded the electromyographic activity of some of the muscles which participate in the movement (deltoid, the elbow flexor brachioradialis and biceps, which acts as a flexor at the elbow and shoulder) and calculated the torques at the two joints from the angular motion and its derivatives.<sup>13</sup>

As can be seen from Fig. 12, there are no obvious abrupt changes either in the torque or in the electromyographic activity which could suggest the presence of segmentation. The data shown in Fig. 12A are from trials in which the subject drew a 'figure 8' on its side ( $\infty$ ) and in Fig. 12B for a 'figure 8' drawn in an oblique plane. The time-scale has been normalized to the duration of one cycle ( $t = 1.0$ ) and the reversal from clockwise to counter-clockwise motion occurs at  $t = 0.5$  and  $t = 1.5$ . Thus, segments begin at time  $t = 0$  and  $t = 1.0$ , and also at  $t = 0.5$ , as indicated by the dashed lines. (In Fig. 12A, there are in fact four segments per cycle, see Fig. 8.) Data for a number of cycles have been averaged. It is evident that EMG

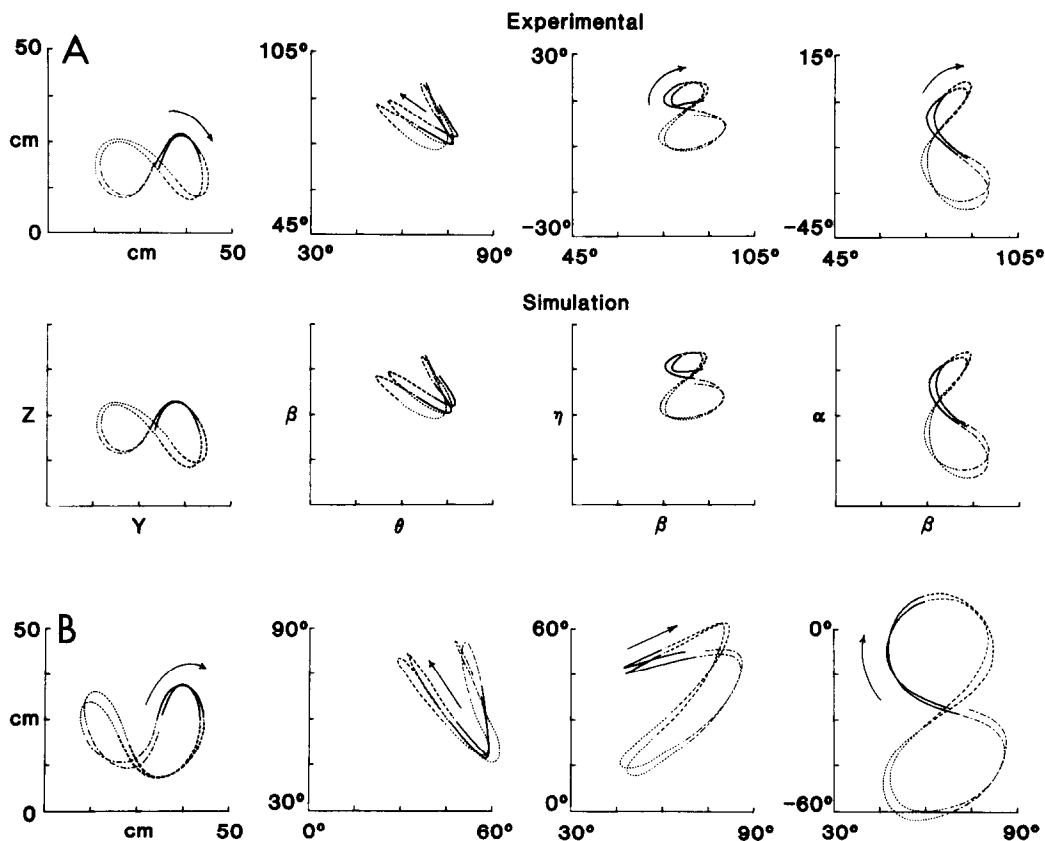


Fig. 8. (A) Comparison of experimental data and the results of a simulation assuming sinusoidal motion of the orientation angles of the arm and forearm for the same trial as in Fig. 7. (B) Experimental data from another subject, the motion of the wrist having a somewhat different form.

activity and torque are modulated in a relatively continuous fashion and that the beginning of a new segment is not marked by any sudden obvious change in the pattern of activity. One other finding is apparent in Fig. 12. The pattern of activation of a given muscle can be very different from task to task and from muscle to muscle. Furthermore, even the timing of peaks in the activity of muscles which have similar actions (i.e. biceps and brachioradialis) can differ substantially (see Fig. 12A, where the second peak in brachioradialis lags that in biceps by more than 100 ms).

#### DISCUSSION

The data presented here support the hypothesis stated in the Introduction, namely that apparently continuous movements are composed of unit segments, each of which constitutes an arc of an ellipse generated according to the rules of the algorithm described there. In fact, these rules were found to be obeyed for planned wrist trajectories different from those used previously for identifying the rules. We performed simulations in which we assumed that each elliptical arc resulted from sinusoidal motion of

the orientation angles at a common frequency. The motivation for assuming sinusoidal angular motion was provided by a mathematical analysis we have presented previously<sup>15,17</sup> and which was summarized in the Introduction. The intent of the simulations was to ascertain the extent to which this assumption gave a satisfactory approximation of the data. In fact we were able to reproduce the essential features of the movement, namely the form of the motion in space, the relationship between curvature and speed of the wrist trajectory and the relationships among the orientation angles constituting the intrinsic coordinate system. Finally, each segment of the wrist trajectory was found to be restricted to one plane only, as predicted by the hypothesis.

A fundamental constraint of the algorithm is that the modulation in the angular elevation of the arm and forearm be close to 180° out of phase.<sup>17</sup> This constraint was obeyed in the present data although the variability in this phase relation was sometimes greater than for circles and ellipses. (However, in one of the subjects this phase relation did differ substantially from 180° when he was asked to draw 'figure 8s'.) As a result of this constraint the slant of the elliptic arc is determined by the phase difference

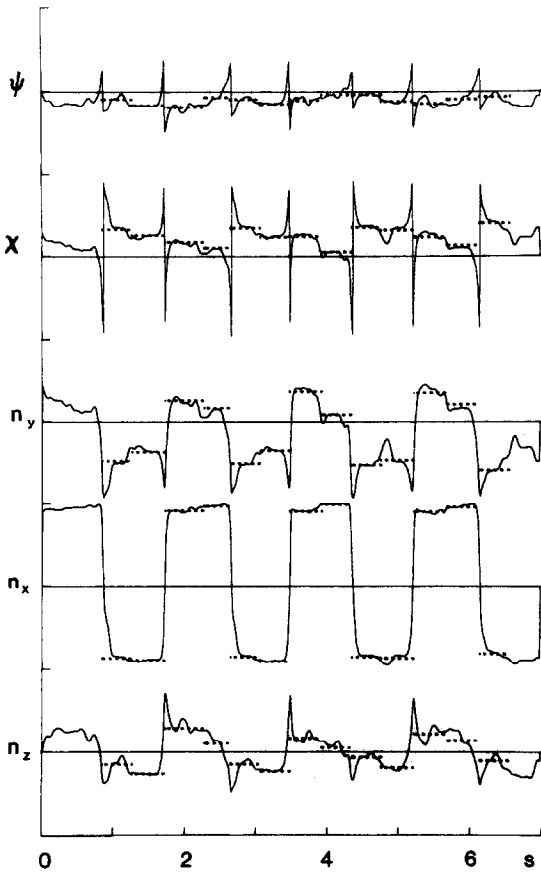


Fig. 9. Changes in the plane of wrist motion. The data are for the same trial as depicted in Figs 7 and 8A.

between yaw and angular elevation of the forearm. These two parameters were always highly correlated and thus this criterion also is satisfied. Finally, the algorithm states that the azimuth of the plane of motion is related linearly to the phase difference between upper arm and forearm yaw angles. Since all movements performed by the subjects were close to the frontal plane (azimuth  $\chi < 30^\circ$ ), the general validity of this relationship could not be tested.

To determine these phase relations we assumed that the motion of each of the orientation angles was sinusoidal during each segment. It should be noted that this assumption was the simplest we could make and that other forms of periodic motion may also conform to the experimental observations. For example, the general criterion for planar wrist motion and for the observed relationship between tangential velocity and curvature is that the second derivative of velocity be parallel to velocity (eq. 8 of Ref. 17). Sinusoidal modulation of velocity is only one particular solution obeying this condition. Similarly, a central tenet of our hypothesis is that there are simple relations between extrinsic and intrinsic parameters of the motion. We have characterized the intrinsic parameters as phase relations between sinusoidal modulations of the orientation angles. However, these parameters could also be represented in terms of the relative timing of the maxima (or minima) of the orientation angles (or their derivatives). If so, the requirement for sinusoidal angular motion could be relaxed. Whether one or the other of these representations is preferable depends exclusively on the manner in which this algorithm is implemented by the

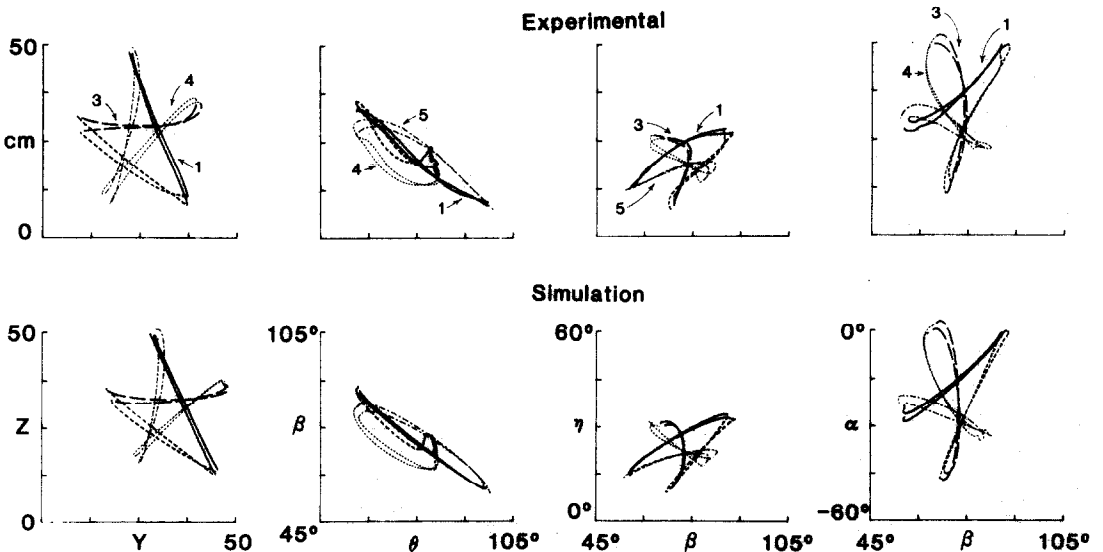


Fig. 10. Comparison of experimental data and results of simulation for a trial in which the subject was asked to draw a five-pointed star repetitively in the frontal plane. Each segment is denoted by a different line symbol; they are numbered consecutively beginning with the downward, rightward stroke (solid traces).

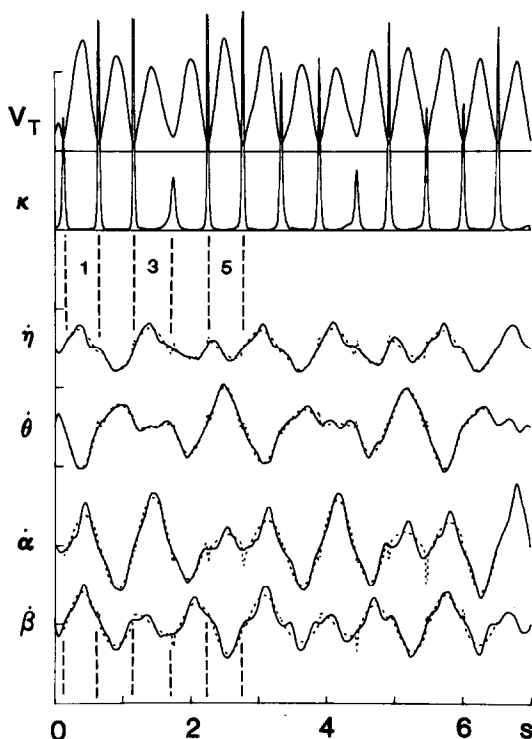


Fig. 11. Variation in tangential velocity, curvature and angular velocities when the subject was asked to draw a five-pointed star. Data are for the same trial as in Fig. 10 and the segments corresponding to one cycle of the movement have been denoted by the vertical dashed lines. Scales per division are:  $V_T$ , 100 cm/s;  $\kappa$ , 2/cm; angular velocities,  $250^\circ/\text{s}$ .

nervous system. Lacking any knowledge on this point, we have chosen the representation which is simplest mathematically.

We also assumed that the motion of the arm consisted of unit segments. Abrupt changes in the plane of motion have been reported previously by Morasso,<sup>11</sup> who asked subjects to generate scribbles in three-dimensional space. He found that the torsion (the rate of change of the plane of motion) exhibited segmented characteristics. A segmentation of the trajectories of handwriting and drawing movements (at points other than cusps, where the tangential velocity is zero) has been suggested explicitly on the basis of abrupt changes in the value of the coefficient relating the tangential velocity and curvature<sup>8,21,22</sup> and in simulation studies of handwriting.<sup>5</sup> Furthermore, on the basis of measures of latency and duration Monsell<sup>10</sup> has presented evidence indicating that speech consists of a sequence of discrete sub-units.

Our data obviously support these points of view, the findings that each segment of the trajectory of the wrist describes a plane and that the plane of motion can change abruptly providing the strongest support. Together with data to be presented in the following paper<sup>18</sup> (showing that subjects are unable to produce wrist trajectories in which the plane of motion

changes smoothly and continuously), they demonstrate that, as required by the algorithm,<sup>17</sup> the motion of the human arm is constrained to be piecewise planar. One can thus expect that some additional constraints are required to join together adjacent segments in a smooth manner. While we have not investigated this problem, one should note that discontinuities in velocity will be smoothed automatically by the viscoelastic properties of the musculoskeletal system and the fact that muscles are capable of generating only a finite amount of force.

Two points remain to be mentioned. The first concerns the possible neural substrates of the algorithm. On this point one might postulate that there should exist neurons whose frequency and/or pattern of discharge is correlated with one of the parameters which are explicit in the algorithm, such as the azimuth or planar elevation of wrist motion. However, the strong possibility exists that such parameters would be encoded not in the discharge of a single neuron (or homogeneous population of neurons) but rather in the behavior of a population each of whose elements have different discharge characteristics. For example, Georgopoulos *et al.*<sup>3,4</sup> have shown that single neurons in motor cortex are broadly tuned to the direction of arm movement in two-dimensional space. Only by making appropriate assumptions were they able to show that the behavior of the population is highly predictive of the direction vector of the movement. Another possibility is that the phase relations we have described are encoded centrally by a population of coupled neural oscillators (e.g. neurons having intrinsic oscillatory properties<sup>6</sup>) whose phasing and frequency can be regulated.

The second point is meant to emphasize the sensorimotor nature of the tasks investigated and the implications of our findings with regard to the perception of ongoing movements on the basis of kinaesthetic information.<sup>15</sup> On this point it should be stressed that the proposed algorithm is transitive, that is, given a desired motion of the wrist it can be used to predict the angular motion of the arm and forearm and, conversely, given the motion of the orientation angles (the intrinsic coordinate system) one can predict the motion of the endpoint (wrist). Thus the algorithm can be utilized both for the generation of arm movements as well as for their perception, elements of the topology of this sensorimotor mapping having been specified previously.<sup>15,17</sup> In short, one can conceive a self-initiated action and its perception to form a functional unit, the proposal being that its unitary nature is provided by a transitive algorithm.

While some consequences of this proposition can ultimately be tested in the case of arm movements, there are a number of fundamental questions which must be resolved. For example, what is the spatial resolution of the hypothesized mapping between intrinsic and extrinsic coordinates? Thus, is the lack of awareness by the subjects of appreciable distortions

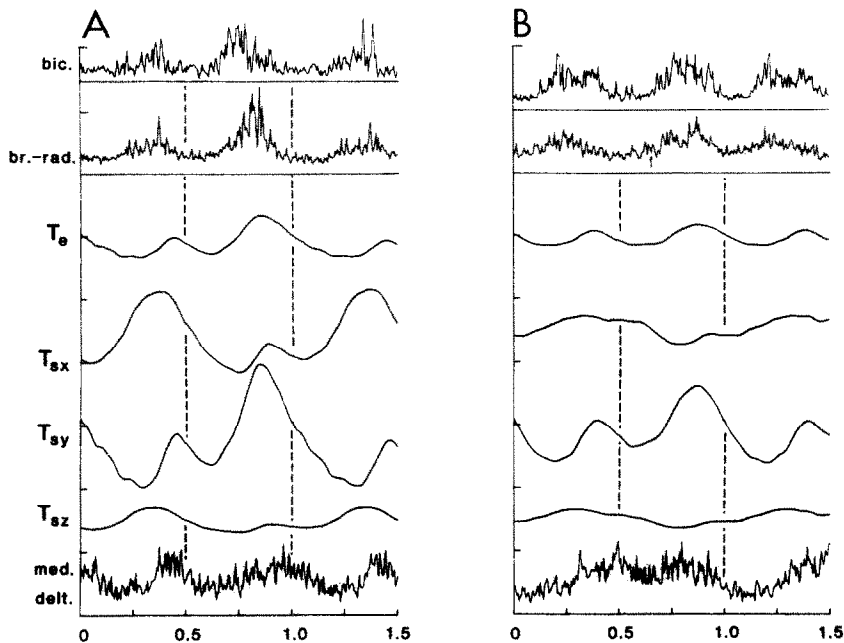


Fig. 12. Torque at the elbow ( $T_e$ ) and at the shoulder ( $T_s$ ) and rectified electromyographic activity of elbow and shoulder muscles during the production of '∞' in (A) and '8' in an oblique plane (B). The components of shoulder torque are illustrated in a frame of reference fixed to the upper arm,  $T_{sx}$  being the torque about the anterior direction when the upper arm is vertical and the arm lies in the sagittal plane,  $T_{sy}$  the torque about the mediolateral direction and  $T_{sz}$  about the vertical. The time-scale is arbitrary, the period of one complete cycle of each movement being unity. According to the criteria used, segmentation of the motion occurs at  $t = 0, 0.5$  and  $1.0$ , as indicated by the vertical dashed lines. The scale for the torques is 10 Nm/division.

in the trajectories of arm movements due to poor spatial resolution during the movements or is it the consequence of the approximations inherent in the algorithm, as we have suggested? Furthermore, what is the perceptual representation of a given movement? On this second question one could suppose that the parameters we have identified (plane of motion and slant) are primitive and that the perceptual representation derived from these parameters is more abstract (e.g. form). This may not be unlikely since the plane

of motion could change by as much as  $25^\circ$  from one segment to the next, yet the subjects were not aware of this fact. Furthermore, such a scheme is similar to what has been proposed for visual processing,<sup>9</sup> namely that the perceived image is constructed out of more primitive elements.

*Acknowledgements*—This work was supported by grants from NSF (BNS-8418539) and from USPHS (NS-15018) and the CNR.

#### REFERENCES

1. Abend W., Bizzi E. and Morasso P. (1982) Human arm trajectory formation. *Brain* **105**, 331–348.
2. Flash T. and Hogan N. (1985) The coordination of arm movements: an experimentally confirmed model. *J. Neurosci.* **5**, 1688–1703.
3. Georgopoulos A. P., Caminiti R., Kalaska J. F. and Massey J. T. (1983) Spatial coding of movement: a hypothesis concerning the coding of movement direction by motor cortical populations. *Exptl Brain Res. Suppl.* **7**, 327–336.
4. Georgopoulos A. P., Kalaska J. F., Caminiti R. and Massey J. T. (1982) On the relations between the direction of two-dimensional arm movements and cell discharge in primate motor cortex. *J. Neurosci.* **2**, 1527–1537.
5. Hollerbach J. M. (1981) An oscillation theory of handwriting. *Biol. Cybern.* **39**, 139–156.
6. Jahnsen H. and Llinás R. (1984) Ionic basis for the electroresponsiveness and oscillatory properties of guinea-pig thalamic neurones *in vitro*. *J. Physiol., Lond.* **349**, 227–247.
7. Lacquaniti, F., Ferrigno G., Pedotti A., Soechting J. F. and Terzuolo, C. (1987) Changes in spatial scale in drawing and handwriting: kinematic contributions by proximal and distal joints. *J. Neurosci.* **7**, 819–828.
8. Lacquaniti, F., Terzuolo C. and Viviani P. (1983) The law relating the kinematic and figural aspects of drawing movements. *Acta psychol.* **54**, 115–130.
9. Marr D. (1982) *Vision*. W. H. Freeman, San Francisco.
10. Monsell S. (1986) Programming of complex sequences: evidence from the timing of rapid speech and other productions. In *Generation and Modulation of Action Patterns* (eds Fromm C. and Heuer H.), *Exptl Brain Res. Suppl.* **15**, 72–86.
11. Morasso P. (1983) Three dimensional arm trajectories. *Biol. Cybern.* **48**, 187–194.

12. Soechting J. F. (1982) Does position sense at the elbow reflect a sense of elbow joint angle or one of limb orientation? *Brain Res.* **248**, 392–395.
13. Soechting J. F. (1983) Kinematics and dynamics of the human arm. Laboratory of Neurophysiology Report, University of Minnesota, Minneapolis.
14. Soechting J. F. (1984) Effect of target size on spatial and temporal characteristics of a pointing movement in man. *Expl Brain Res.* **54**, 121–132.
15. Soechting J. F., Lacquaniti F. and Terzuolo C. A. (1986) Coordination of arm movements in three-dimensional space. Sensorimotor mapping during drawing movement. *Neuroscience* **17**, 295–311.
16. Soechting J. F. and Ross B. (1984) Psychophysical determination of coordinate representation of human arm orientation. *Neuroscience* **13**, 595–604.
17. Soechting J. F. and Terzuolo C. A. (1986) An algorithm for the generation of curvilinear wrist motion in an arbitrary plane in three-dimensional space. *Neuroscience* **19**, 1393–1405.
18. Soechting J. F. and Terzuolo C. A. (1987) Organization of arm movements in three-dimensional space. Wrist motion is piece-wise planar. *Neuroscience* **23**, 53–61.
19. Sokolnikoff I. S. and Redheffer R. M. (1958) *Mathematics of Physics and Modern Engineering*, Chapter 4. McGraw-Hill, New York.
20. Terzuolo C. A. and Viviani P. (1979) The central representation of learned motor patterns. In *Posture and Movement* (eds Talbott R. E. and Humphrey D. R.), pp. 113–121. Raven Press, New York.
21. Viviani P. and Cenzato M. (1985) Segmentation and coupling in complex movements. *J. exp. Psychol. hum. Percept. Perf.* **11**, 828–845.
22. Viviani P. and Terzuolo C. (1982) Trajectory determines movement dynamics. *Neuroscience* **7**, 431–437.

(Accepted 20 February 1987)